Neurochemistry International 129 (2019) 104511

Contents lists available at ScienceDirect

Neurochemistry International

journal homepage: www.elsevier.com/locate/neuint

Maternal exposure to swainsonine impaired the early postnatal development of mouse dentate gyrus of offspring

Mengmeng Liu[a], Mingrui Xu[b], Mengli Wang[a], Shuzhong Wang[a], Kaikai Li[a], Xinran Cheng[a], Yongji Wu[a], Yi Wang[c], Xiaoyan Zhu[a,**], Shanting Zhao[a,*]

[a] College of Veterinary Medicine, Northwest A & F University, Yangling, Shaanxi, 712100, PR China
[b] College of Food Science and Engineering, Northwest A&F University, Yangling, Shaanxi, 712100, PR China
[c] Shenzhen Key Laboratory of Food Biological Safety Control, Shenzhen Research Institute of Hong Kong Polytechnic University, Shenzhen, 518057, PR China

ARTICLE INFO

Keywords:
Swainsonine
Dentate gyrus
Neurogenesis
Neuronal migration
Postnatal *in vivo* electroporation

ABSTRACT

Neurogenesis in the dentate gyrus (DG) plays a key role in the normal of structure and function of the hippocampus—learning and memory. After eating the locoweeds, animals develop a chronic neurological disease called "locoism". Swainsonine (SW) is the main toxin in locoweeds. Studies have shown that SW induces neuronal apoptosis *in vitro* and impairs learning and memory in adult mouse. The present study explored effects of SW exposure to dams on the postnatal neurogenesis of DG of offspring. Pregnant ICR mice were orally gavaged with SW at a dose of 0, 5.6 or 8.4 mg/kg/day from gestation day 10 to postnatal day (PND) 21, respectively. We found that SW impaired the proliferation capacity of neural progenitor cells in the DG so that the number of newborn cells was reduced at PND 8. Using the postnatal *in vivo* electroporation, we showed that the dendritic branching and total length of granule cells were significantly decreased due to SW exposure. In addition, on PND 21, the density of NeuN-positive and Reelin-positive interneurons increased in the hilus, implying the disorder of neuronal migration. These results suggest that maternal exposure to SW, the neurogenesis of DG on offspring was disrupted, finally leading to the functional disorder of DG.

1. Introduction

Locoweeds, from *Oxytropis and Astragalus*, are a great threat to grass farming in the livestock industry (Lu et al., 2014a; Wu et al., 2014). Swainsonine (SW) is the main toxin in locoweeds (Obeidat et al., 2005; Yu et al., 2010). Studies have shown that SW can inhibit α-mannosidase and finally result in the formation of vacuoles in different kinds of cells (Armien et al., 2007; Wang et al., 2013). SW-poisoning animals do have clinical symptoms of nervous system damage such as mentally depressed, drowsy and ataxia (Armien et al., 2011; Dantas et al., 2007; Driemeier et al., 2000; Wu et al., 2014). Once the poisoned animals stop feeding on locoweeds, the structure and function of cells in most systems and organs generally recover within a few days to several weeks (Armien et al., 2011; Dantas et al., 2007; Wu et al., 2014). However, the nervous system damage is not easy to repair, and even lead to permanent neurological disorders. These imply that the nervous system is more sensitive to SW than other systems.

In rodents, the developing central nervous system has a critical period called brain growth spurt–from the end of pregnancy to the first 2–3 weeks after birth; in humans, the corresponding period begins at the final trimester of pregnancy and lasts 2 years after birth (Byrnes et al., 2001). During this time, the brain exhibits rapidly substantial neurogenes and has a high degree of plasticity, laying foundations for the normal structure and function of the brain. The hippocampal dentate gyrus (DG) is one of regions where neurogenesis occurs during development and continues, at a slower rate, into adulthood. Hippocampus is primarily composed of DG, the cornus ammonis (CA) and the subiculum, and critical for certain forms of learning and memory (Squire and Zola-Morgan, 1991). It has been confirmed that a positive correlation between neurogenesis in DG and the performance of the animal on behavioral tasks (Kempermann et al., 1997; van Praag et al., 1999).

DG development begins from around gestation day (GD) 15 and lasts until the postnatal day (PND) 14-21, which is accomplished by multiple spatiotemporally regulated developmental processes involving proliferation, migration, differentiation, and morphological change of neural stem cells (NSCs) (Altman and Bayer, 1990a, b; Li and Pleasure, 2005). NSCs including radial glial cells (RGCs) and intermediate neural

* Corresponding author.
** Corresponding author.
E-mail addresses: xyzhu0922@163.com (X. Zhu), shantingzhao@hotmail.com (S. Zhao).

https://doi.org/10.1016/j.neuint.2019.104511
Received 21 March 2019; Received in revised form 22 July 2019; Accepted 23 July 2019
Available online 23 July 2019

progenitors (INPs) migrate toward the hilus of DG and form a proliferative zone, called the subgranular zone (SGZ), at the border between the hilus and the granular cell layer (GCL) in the second postnatal week (Li et al., 2009; Li and Pleasure, 2005), and neurogenesis in the SGZ contributes to be persistent throughout life. RGCs produce INPs and further differentiate into granule cells (GCs) that are integrated into the GCL. However, only some newborn GCs can migrate into the normal position of the GCL to finish the functional demand (Dupret et al., 2007; Kee et al., 2007). During the process, reelin signaling participates in the final destination of GCs (Brunne et al., 2013). A great deal of neuropathological defects that cause high cognitive dysfunction are accompanied by abnormal hippocampal neurogenesis and plasticity (Xu et al., 2015). Seizures have effects on the development of hippocampal neurogenesis and irregular hilar basal dendrites (Hattiangady and Shetty, 2010; Jessberger et al., 2007). Normally, GCs develop dendrites towards the molecular layer (ML) of DG and send axons through the hilus. In contrast, dendrites from seizure-induced GCs appear to grow the hilus rather than the ML. In addition, results have demonstrated that factors that interfere with neuronal production (eg, after birth or adult) may have serious implications on hippocampus-dependent function (Kempermann and Gage, 2002; Young et al., 1999). Therefore, neurogenesis in the DG plays a key role in the normal of structure and function of the hippocampus.

The study has shown that SW can cause apoptosis of dopaminergic neurons in the midbrain (Li et al., 2012). Treatment with SW can affect the growth of rat neuronal processes, the expression of Golgi mannosidase II and lead to neuronal apoptosis (Lu et al., 2013, 2014b). In addition, our previous study found that SW significantly inhibited adult neurogenesis in hippocampus and affected spatial learning and memory in mice (Wang et al., 2015). Here, at the GD 10, dams were exposed to SW and continued until the PND 21 to investigate the effects of SW on the neurogenesis of DG. Our results showed that SW exposure impaired proliferation of RGCs and INPs and reduced the number of newborn cells in DG on offspring at PND 8. Using postnatal *in vivo* electroporation and western blot, we found that SW affected dendritogenesis of GCs and reduced the expression level of spinophilin in neonatal hippocampus. Interestingly, the number of $NeuN^+$ and $Reelin^+$ cells in hilus significantly increased, suggesting the migration defect of newborn neurons. In addition, by western blot analysis, we found the relative expression level of NeuN with treatment of 8.4 mg/kg SW obviously decreased in the whole neonatal hippocampus, suggesting that SW did disrupt the development of hippocampus. These results indicated that exposure of dams to swainsonine affected early development of dentate gyrus on offspring.

2. Materials and methods

2.1. Chemical reagents and antibodies

Swainsonine (SW, purity > 99.8%), propidium iodide (PI) and 5′-Bromo-2′-deoxyuridine (BrdU) were from Sigma. 4′, 6′-diamidino-2-phenylindole (DAPI) was purchased from Abcam. For immunofluorescence staining, the primary antibodies used in the present study were as follows: rabbit anti-BLBP (Millipore, ABN14, 1:500), rat anti-BrdU (Santa Cruz Biotechnology, sc-56258 1:500), rabbit anti-GFP (Thermo Fisher Scientific, G10362, 1:200), rabbit anti-prox1 (Millipore, AB5475, 1:1000), mouse anti-NeuN (Abcam, ab104224, 1:1000) and rabbit anti-Tbr2 (Abcam, ab183991, 1:200). The following second antibodies (1:300 for all) were purchased from Abcam: Alexa Fluor 488-conjugated donkey anti-rabbit IgG (ab150073), Alexa Fluor 488-conjugated goat anti-rat IgG (ab150157) and Alexa Fluor 647-conjugated goat anti-rat IgG (ab150159). For immunoblot analysis, the primary antibodies were as follows: mouse anti-synaptophysin (Abcam, ab8049, 1:2000), rabbit anti-spinophilin (Abcam, ab18561, 1:2000), mouse anti-GAPDH (Cell Signaling Technology, D4C6R, 1:2000) and mouse anti-NeuN (Abcam, ab104224, 1:2000). And HRP-coupled secondary antibodies (goat anti-mouse IgG, ab6789, Abcam; goat anti-rabbit IgG, ab6721, Abcam) from the corresponding species were used in a dilution of 1:2000.

2.2. Animals and drug treatment

ICR mice aged 3 months old came from the Animal Experimental Center of Xi'an Jiaotong University (Xi'an, China) and adapted to the environment for 7 days. All mice were housed at a room with standard light (12 h light/12 h dark) and appropriate temperature and free to gain food and water. ICR mice were caged at a ratio of one male to two females, and the day of appearance of vaginal plug was deemed to the GD 0.

SW was dissolved in 0.9% NaCl and the appropriate doses for this study were determined based on a previous study (Wang et al., 2015) and preliminary experiments. In this study, only one pregnant mouse was placed in one cage. The 18 pregnant mice were randomly and equally divided into three groups, and then they began to be orally administered with vehicle or SW at the dose of 0, 5.6, 8.4 mg/kg/day from GD 10 to PND 21. The number of pups was removed to 10 at PND 2. All animal experiments were carried out by the Animal Care Commission of the College of Veterinary Medicine, Northwest A&F University (certificate no.: SCXK [SHAAN] 2017 − 003) in accordance with ARRIVE guidelines (https://www.nc3rs.org.uk/arrive-guidelines).

2.3. Postnatal in vivo electroporation

Postnatal *in vivo* electroporation was applied according to the previously published method (Ito et al., 2014). In short, the plasmid vector–pCAG-MCS-GFP (GFP) was extracted by the Endo-Free Plasmid Maxi Kit (Omega). And GFP (3 μg/μL) mixed with 0.1% Fast Green (Sigma) was injected into the lateral ventricle of the right brain of four pups per litter at PND 0 through a special glass micro-capillary by using an electrical pulse of 950 ms interval of five pulses at 100 V (ECM 830, BTX). After the operation, pups were placed on a heating pad at 37 °C for a few minutes before returning to their mothers for keeping them alive. These brains were acquired at PND 21 and fixed with 4% paraformaldehyde (PFA) for at least 3 days.

2.4. BrdU labeling assay

The BrdU labeling experiment was described in the previous article (Xu et al., 2018). In brief, pups were intraperitoneally injected with BrdU (50 mg/kg) at PND 8 and sacrificed after 2 h to study cell proliferation. In addition, to further study the early development of postnatal DG, newborn pups were forced to inject once with BrdU at PND 2 and sacrificed at PND 8 and their brains were fixed in 4% PFA for at least 24 h.

2.5. Tissue preparation and immunofluorescence staining

The fixed brains were embedded in 4% agarose and then using a vibration microtome (VT1000S, Leica) subjected to a continuous coronal section with a thickness of 50 μm or 200 μm. After washing three times in 0.1 M phosphate buffer (PB, pH 7.4), sections were incubated with the primary antibody dissolved in a diluting agent (4% BSA, 0.3% Triton X-100 and 1% normal goat serum). For BrdU immunostaining, free-floating slices were pre-treated with 2 M HCl for 30 min at 37 °C and neutralized three times for 10 min each time with 0.1 M borate buffer (pH 8.5). These slices were incubated with the rat anti-BrdU. All slices were then rinsed three times in 0.1 M PB and then incubated in species-specific secondary antibodies for 4 h at room temperature (RT). Cell nuclei were countstained with DAPI or PI for 20 min, and slices were mounted with Dako. All images were taken using a laser-scanning confocal microscope (TCS SP8, Leica).

2.6. Immunoblot analysis

The hippocampus was extracted in ice-cold RIPA-lysis buffer with 1% protease inhibitor (Roche) and phosphatase inhibitor cocktails (Roche) according to the previous study (Li et al., 2017). These samples were separated by 10% Bis-Tris, with SDS-PAGE running buffer and transferred electrophoretically to polyvinylidene fluoride (PVDF) membranes (Millipore). After 5% fat-free milk for 2 h at RT, primary antibodies were incubated at 4 °C overnight. HRP-coupled secondary antibodies (goat anti-mouse IgG, ab6789, Abcam; goat anti-rabbit IgG, ab6721, Abcam) from the corresponding species were used in a dilution of 1:2000. All experiments were repeated at least three times. These specific protein bands on the PVDF membranes (Millipore) were visualized via enhanced chemiluminescent detection and photographed with a chemiluminescent imaging system (Beijing Sage Creation company, China). For densitometric quantifications, these images were analyzed with the Image J software.

2.7. Quantification and morphological analysis

For quantification of the number of labeled cells, three coronal slices with a thickness of 50 μm per animal were counted at the same anatomical level (Bregma −1.70 mm to −1.94 mm) with reference to the research article (Kadam et al., 2013) and brain map (Paxinos and Franklin, 2001). To study cellular proliferation in DG, the number of $BrdU^+$ cells was counted. For $BrdU^+$ and $Prox1^+$ double labeled cells, the number of cells in the GCL and hilus was analyzed, respectively. To further study the early development of postnatal DG, the number of $BrdU^+$ cells of GCL per 0.01 mm^2 was analyzed. For quantification of RGCs and INPs, the number of $BLBP^+$ $BrdU^+$ and $Tbr2^+$ $BrdU^+$ double labeled cells was counted in the GCL plus SGZ, respectively.

For morphological analysis, three coronal slices with a thickness of 200 μm per animal were counted at the same anatomical level (Bregma −1.70 mm to −2.30 mm) according to the previous study (Campbell et al., 2008) and brain map (Paxinos and Franklin, 2001). 10–15 GFP-labeled GCs per pup were measured. The Neuron J plug-in was used to analyze the total length and the number of terminal branches of dendrites of GCs and the Sholl analysis plug-in was to do the concentric circle analysis of dendrites (Ferreira et al., 2014; Meijering, 2010). To analyze the density, all visible spines in the terminal branch of dendrites at the outer ML and MFB (2–5 μm, > dendrites in diameter) in the hilus were counted by Image J and the plug-in Neuron J. At least 10 fragments were analyzed for each animal.

2.8. Statistical analysis

In this study, all slices were photographed and subsequently analyzed by Image J (https://imagej.net/, RRID: SCR_003070). Data analysis was executed by the software SPSS Statistics 21.0 (http://www-01.ibm.com/software/uk/analytics/spss/, RRID: SCR_002865). Statistical analysis of data was by one-way ANOVA with Dunnett's test or Tamhane's T2 test. For the Sholl analysis, a two-way ANOVA followed by a Dunnett's test was used to measure repeated data. All charts were completed by GraphPad Prism 5.0 software (http://www.graphpad.com/, RRID: SCR_002798). Statistical results were expressed as mean ± standard deviation (SD) or standard error (SEM), and the value of $p < 0.05$ was statistically significant.

3. Results

3.1. SW exposure did not affect the body weight of dams as well as the body weight and brain of their offspring

No significant difference was found in the body weight of dams between the control group and the SW-treated groups (Fig. 1a). Brain weight (Fig. 1b), body weight (Fig. 1c) and the ratio of body weight to brain weight of the offspring mice (Fig. 1d) did not show significant difference between the control group and the SW-treated groups.

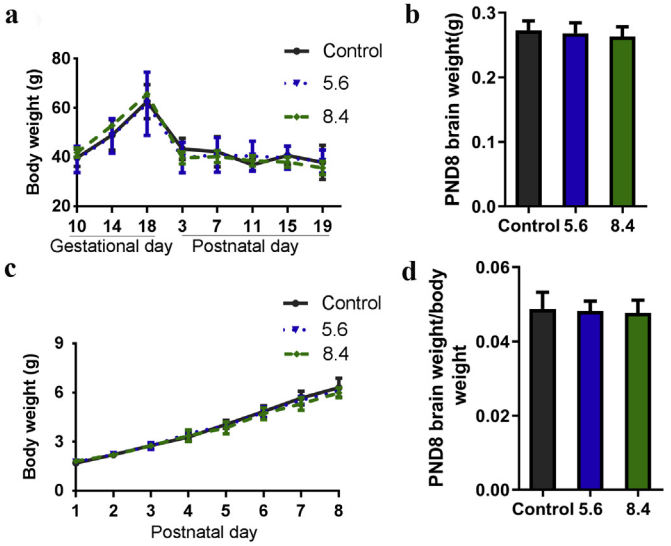

Fig. 1. Exposure to SW did not affect the body weight of dams, brain weight, body weight and the ratio of brain weight to body weight of offspring. **a** Body weight of dams. ($n = 6$ per group) **b** Brain weight of offspring at PND 8 ($n = 9$ per group). **c** Body weight of offspring ($n = 9$ per group). **d** The ratio of brain weight to body weight at PND 8 ($n = 9$ per group). No difference was found between the control group and SW-treated groups. *PND* postnatal day. Data were presented as the mean ± SD.

3.2. SW exposure impaired the early development of postnatal DG

It is well known that as the RGCs proliferate to expand the DG, they produce INPs and later migrate to the hilus of the DG to give rise to the prospero homeobox 1-positive ($Prox1^+$) cells (Altman and Bayer, 1990a, b; Li et al., 2009; Li and Pleasure, 2005). We analyzed cell proliferation in DG by double labeling with BrdU and Prox1 (Fig. 2a and b) and found that compared with that in control group, the number of $BrdU^+$ cells was significantly decreased in SW-treated groups (Fig. 2e) in the whole DG. The number of $Prox1^+$ $BrdU^+$ double-labeled cells in GCL showed no significant difference between control and SW-treated groups (Fig. 2g), whereas the number of $Prox1^+BrdU^+$ double-labeled cells in hilus of the SW-treated groups was significantly reduced (Fig. 2f), indicating that SW exposure inhibited the proliferation of neural progenitor cells in DG.

In order to investigate the effect of SW on the early development of postnatal DG, we injected BrdU at PND 2 and followed by fixation and staining at PND 8 (Fig. 2d). The density of $BrdU^+$ cells in GCL per 0.01 mm^2 was approximately 39 in the control group and only 29 and 26 $BrdU^+$ cells were found in the 5.6 mg/kg and 8.4 mg/kg groups, respectively (Fig. 2h). These results indicate that SW impaired the early development of postnatal DG.

3.3. SW exposure impaired the proliferation capacity of RGCs and INPs in DG

We have shown that SW exposure reduced the number of newborn cells. To study the reasons for the decrease in the number of newborn cells, we used antibodies against brain lipid binding protein (BLBP) and T-box brain gene 2 (Tbr2) to label RGCs (Fig. 3a and b) and INPs (Fig. 3d and e), respectively. The results showed that the number of proliferating RGCs ($BLBP^+$ and $BrdU^+$) in the SW-treated groups was less than that in control group (Fig. 3c). Moreover, SW strikingly decreased the number of proliferating INPs ($Tbr2^+$ and $BrdU^+$) in GCL (plus the SGZ) in the SW-treated groups (Fig. 3f). These results implied

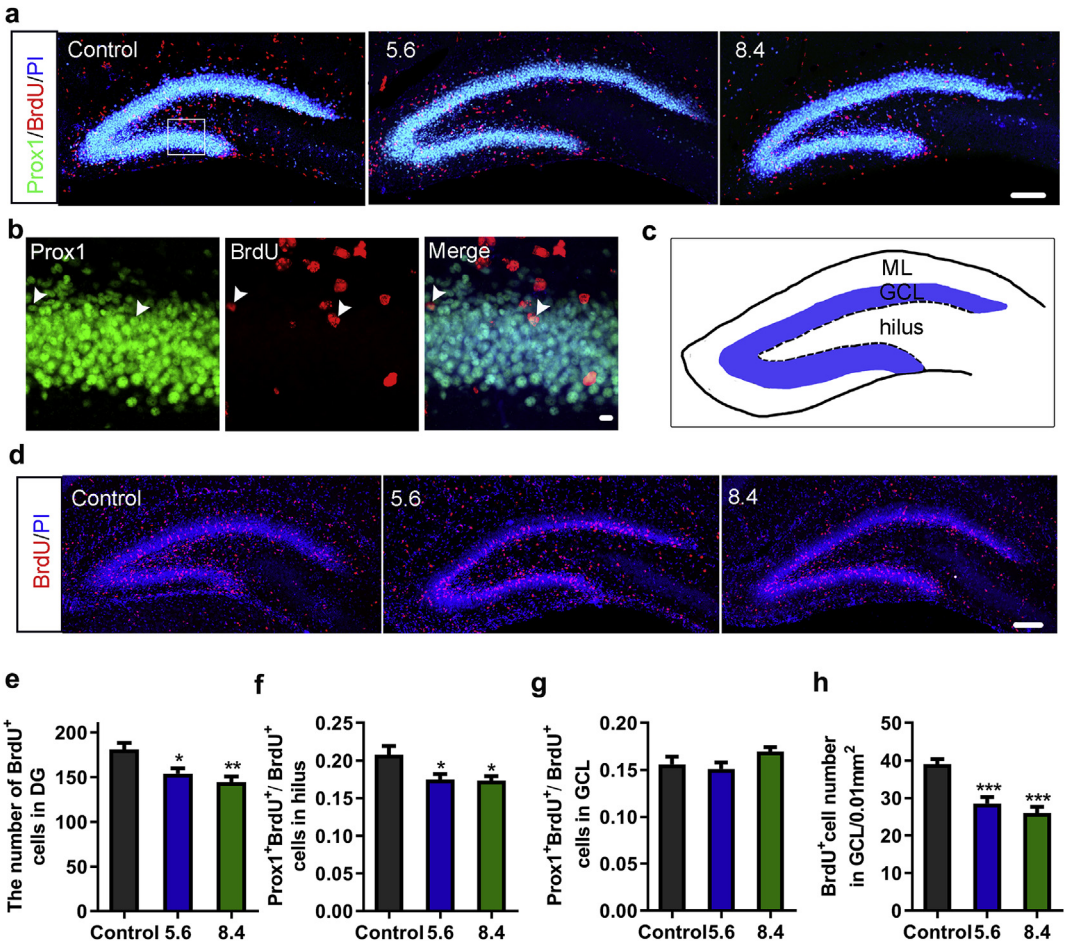

Fig. 2. Developmental SW exposure decreased the number of newborn cells in DG at PND 8. **a** Representative immunofluorescence images showing newborn cells labeled by BrdU (red) and Prox1 (green) in DG at 2 h after BrdU injection at PND 8. The sections were counterstained with PI (blue). **b** High magnifcation of newborn cells (*arrowhead*) from the boxed area in the control group (**a**). **c** Schematic illustration of the DG. The dashed line at the border between the hilus and the GCL represents the subgranular zone (SGZ). **d** Images showed newborn cells labeled by BrdU (red) and PI (blue) in GCL at 6 days after BrdU injection at PND 2. **e-g** Quantification of BrdU-labeled newborn cells in the whole DG (**e**) and $BrdU^+$ $Prox1^+$ cells in the hilus (**f**) and GCL (**g**). **h** Quality analysis of BrdU-labeled newborn cells per 0.01 mm^2 in GCL. The data were presented as mean ± SEM. $*p < 0.05$, $**p < 0.01$ and $***p < 0.001$ vs. the control group ($n = 6$ for each group). *Scale Bars* 100 μm in **a**, **d**, 8 μm in **b**.

that SW caused a decline in the proliferative capacity of RGCs and INPs, thus leading to the disorder of early development of postnatal DG.

3.4. Effects of SW exposure on dendritic development of GCs and synaptic structure in hippocampus during early postnatal development

Postnatally, plenty of GCs are born and begin to develop (Altman and Bayer, 1990a). We further investigated the effects of SW exposure on dendritic development of GCs using postnatal *in vivo* electroporation (Fig. 4a, c). We found that the total length of dendrites (Fig. 4d) and the number of terminal branch tips (Fig. 4e) of GCs on PND 21 were significantly reduced in the SW-treated groups compared with those in control group. The number of intersections between dendrites and concentric circles was shown by the Sholl analysis (Fig. 4b). Results showed that the number of intersections was significantly different between the SW-treated groups and the control one (Fig. 4g), indicating that SW impaired dendritic development of GCs in DG.

Spines and MFB of GCs are important components to form synapses with their projecting neurons and target neurons. To further study the effect of SW on development of dentate GCs, we analyzed the density of spines on the terminal branch of the dendrites in ML (Fig. 4f) and MFB (Fig. 4h) in the hilus. No difference in density of spines and MFB was found between the treated groups and the control group (Fig. 4i and j). However, we studied the expression levels of synaptophysin and spinophilin in hippocampus (Fig. 4k) and found that the level of spinophilin (Fig. 4l, m) significantly reduced with the 8.4 mg/kg SW-treated group compared to the control one. Therefore, exposure SW to dams could impair dendritic development and synaptic formation in the hippocampus of offspring.

3.5. The number of $NeuN^+$ cells and interneuron subpopulations in the hippocampus at PND 21 after SW exposure during early postnatal development

γ-aminobutyric acid (GABA) is considered to be the major neurotransmitter of DG interneurons, and its synthetases, glutamate decarboxylase (GAD) 67 and 65, are markers of GABAergic interneurons (Houser, 2007). The majority of GABAergic interneurons produce Reelin or calcium-binding proteins, such as parvalbumin (PVALB), and regulate the proliferation, migration and differentiation of neural progenitor cells, as well as the neurotransmitter release between neurons (Houser, 2007). On PND 21, in the 8.4 mg/kg SW-treated group, the density of $NeuN^+$ and $Reelin^+$ cells in the hilus showed significant increase (Fig. 5a, b, c, d). No significant difference in the numbers of $GAD67^+$ and $PVALB^+$ interneurons in the hilus were found in any treatment group compared with those in control group (Fig. 5g, h, i, j). In addition, compared with the control group, the expression level of NeuN significantly reduced in the 8.4 mg/kg SW-treated group (Fig. 5e

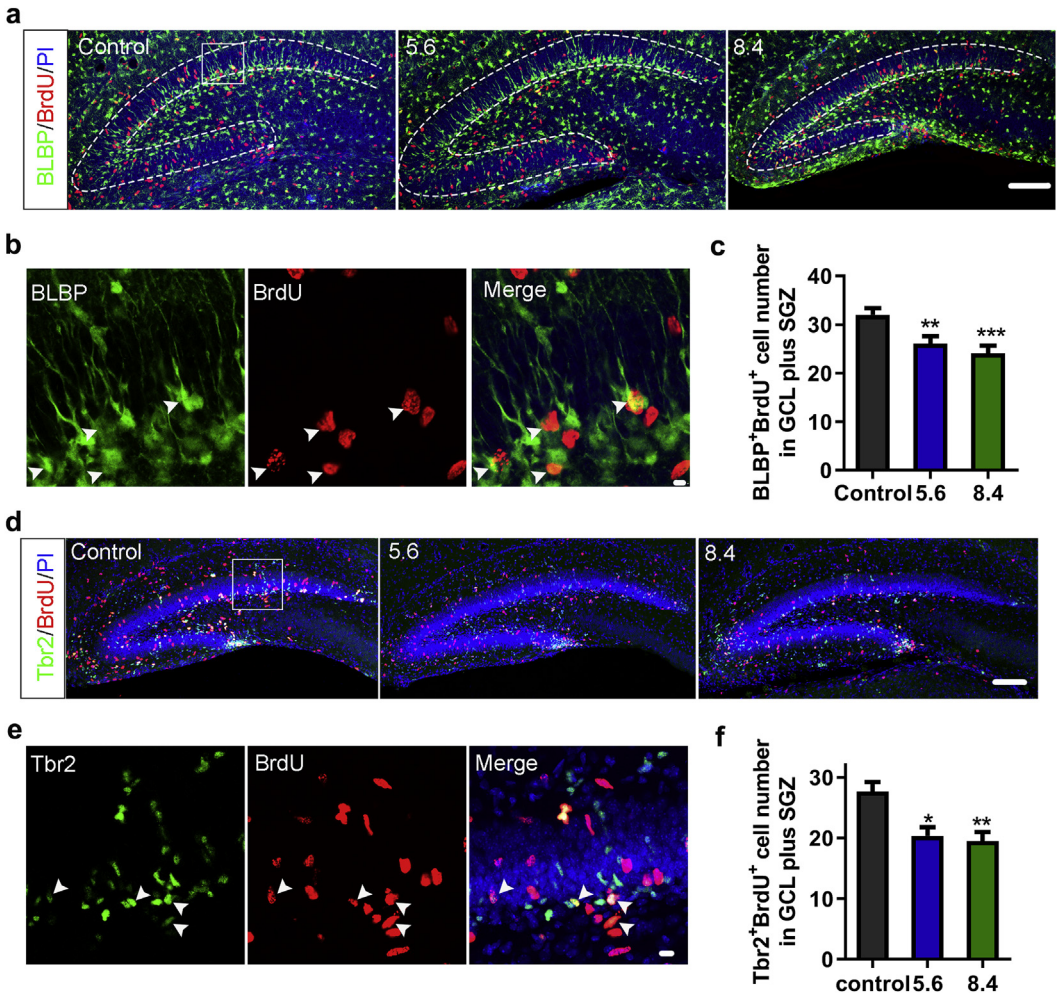

Fig. 3. SW administration reduced the number of proliferating RGCs and INPs in DG. **a** Immunostaining for proliferating RGCs with BLBP (green), BrdU (red), and PI (blue) in the DG of control and SW-treated groups at 2 h after BrdU injection at PND 8. **b** High magnifcation of proliferating RGCs ($BLBP^+BrdU^+$) (*arrowhead*) from the boxed area in the control group (**a**). **c** Quality analysis of the number of $BLBP^+BrdU^+$ cells in GCL plus SGZ. **d** Images showed proliferating INPs labeled by Tbr2 (green), BrdU (red) and PI (blue) in the DG at 2 h after BrdU injection at PND 8. **e** High magnifcation of proliferating INPs ($Tbr2^+BrdU^+$) (*arrowhead*) from the boxed area in the control group (**d**). **f** Quantification of $Tbr2^+BrdU^+$-labeled proliferating INPs in GCL plus SGZ. The data were presented as mean ± SEM. $^*p < 0.05$, $^{**}p < 0.01$ and $^{***}p < 0.001$ ($n = 6$ for each group). *Scale Bars* 100 μm in **a**, **d**, 5 μm in **b**, 10 μm in **e**.

and f).

4. Discussion

SW is the main toxic ingredient in locoweeds, causing serious loco disease ("locoism" or "pea struck") characterized by weight loss, altered behavior, depression, abortion, birth defects, and even death (Stegelmeier et al., 1999). SW has a molecular weight of 173, smaller than that of pathogens so that it can pass placental barrier freely to embryos. Here, we exposed SW to dams to study neurotoxicity on DG of their offspring, including cell proliferation and development during the early postnatal neurogenesis.

Weight loss is one of the characteristics of SW after locoweed poisoning. In this study, dams and their offspring after oral administration of SW, compared to that of control group, the body weight in the SW-treated groups was not significantly reduced. Locoweed poisoning is generally chronic and cumulative, and toxic symptoms are observed after a few weeks of locoweed feeding (Stegelmeier et al., 1995). It may be due to the fact that exposure time of SW and accumulated amount of SW were not enough to affect the body weight in this study.

NSCs persist to produce neurons, with the entire formation of the DG of hippocampus in the first two weeks after birth (Altman and Bayer, 1990a; Li et al., 2009; Mathews et al., 2010). Here, we found that SW exposure apparently decreased the number of $BrdU^+$ cells in DG, suggesting that SW did impair the proliferation of NSCs in DG. During development of DG, GCs are produced from stem cells located in the hilus at PND 8. We used Prox1, a specific marker of dentate GCs in the hippocampus (Ming and Song, 2011; Mateus-Pinheiro et al., 2018), and BrdU double-labeling to represent newborn cells with fate determined as GCs. Statistically, it was found that after SW exposure, the number of $Prox1^+$ $BrdU^+$ cells was significantly decreased in the hilus and did not change in the GCL, suggesting that SW mainly affected the generation of neurons.

During the early development of DG, RGCs and INPs are located and proliferate in hilus. The newly generated neurons migrate toward GCL and gradually differentiate into GCs and finally settle in GCL. We have shown that SW exposure decreased the number of $BrdU^+$ neurons. Did SW directly affect the proliferation of RGCs and INPs or reduce the number of RGCs and INPs, resulting in the reduction of newborn GCs? We labeled RGCs and INPs with BLBP and Tbr2, respectively and Tbr2 appears constrained to a future neuronal fate (Hodge et al., 2008; Steiner et al., 2006). Results showed that with SW exposure, the number of proliferating RGCs ($BLBP^+$ $BrdU^+$) and INPs ($Tbr2^+$ $BrdU^+$) was reduced and RGCs were less than INPs. This implied that SW reduced the generation of GCs by affecting stem cells, and RGCs were more susceptible to SW than INPs.

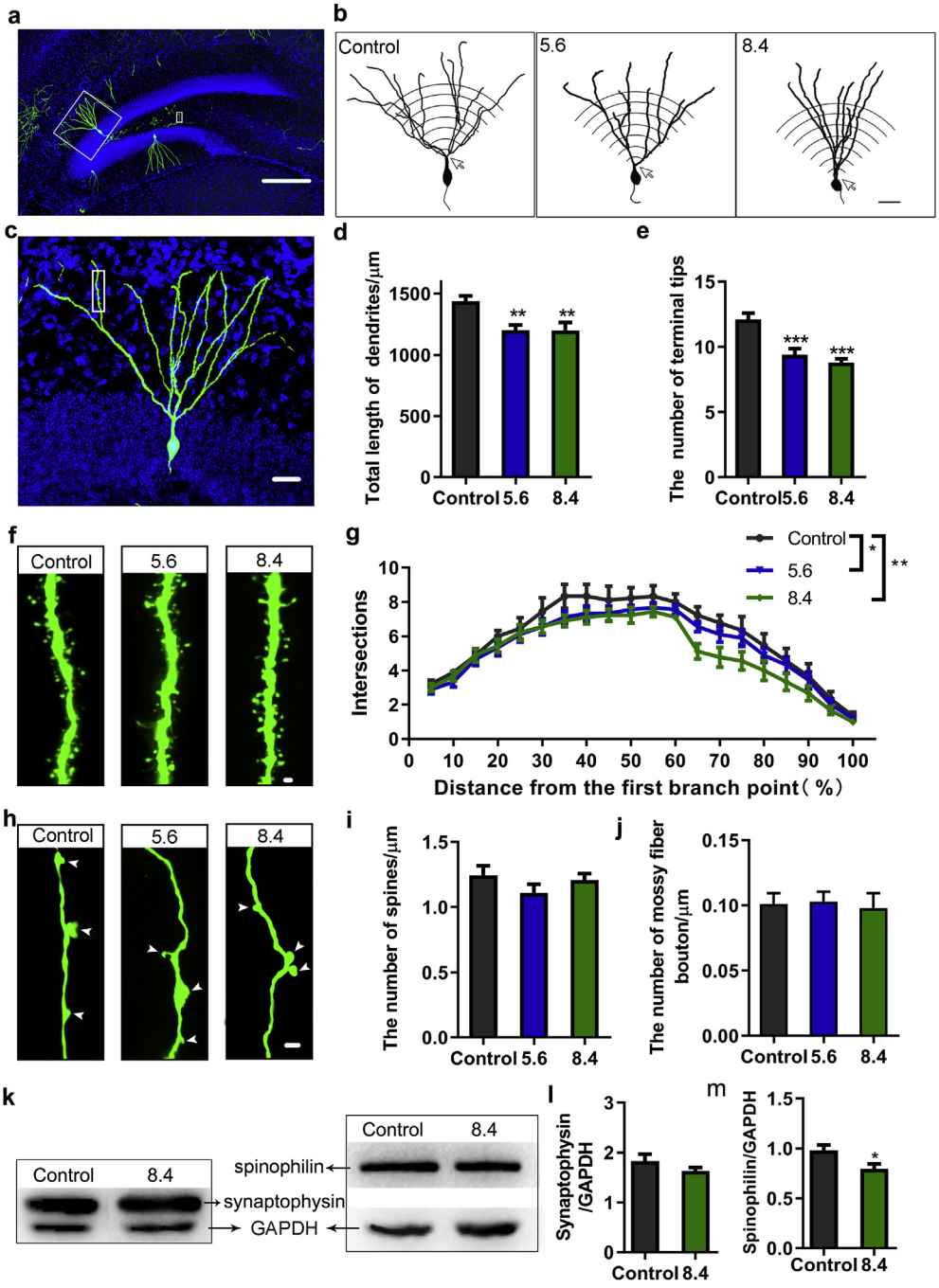

Fig. 4. SW exposure impaired dendritic development of GCs and synaptic structure in hippocampus during early postnatal development. **a** Representative images for GFP-labeled GCs (green) in DG at PND 21 after postnatal *in vivo* electroporation at PND 0. Cell nuclei were counterstained with DAPI (blue). **c** High magnifcation of the GFP^+ GC from the boxed area in the control group (**a**). **b** Illustration of GCs of control and SW-treated groups. The number of intersections between dendritic sections and concentric circles was calculated by the Sholl analysis. The center of the concentric circles was located at the first branch point (*arrow*) of the dendrite. **d-e** Quantification of the total length (**d**) and the number of terminal tips (**e**) of dendrites of the GFP^+ GCs. **g** Sholl analysis of dendrite complexity between control and SW exposure groups. **f** Representative images for spines of GFP-labeled GCs located at the terminal branch of the dendrites in ML, as shown in **c**, the rectangular box in the ML. **h** Representative images for mossy fiber boutons (MFB, *arrowhead*) of GFP-labeled GCs located at the hilus, as shown in **a**, a small rectangular box in the hilus. **i-j** Quality analysis of the density of spines (**i**) and MFB (**j**) on GCs. **k** Immunoblot analysis for spinonphilin and synaptophysin expression levels after treatment with 8.4 mg/kg SW compared with control hippocampus. The GAPDH antibody was used to control loading. **l-m** Densitometric quantification showing spinonphilin (**l**) or synaptophysin (**m**)/GAPDH intensity ratios. Data were presented as mean ± SEM. $^*p < 0.05$, $^{**}p < 0.01$ and $^{***}p < 0.001$ ($n = 9$ for each group). *Scale Bars* 250 μm in **a**, 25 μm in **b**, **c**, 1 μm in **f**, 3 μm in **h**.

We have shown that the decrease of neurons was due to the decline of proliferation capacity of NSCs. In this study, we injected BrdU on PND 2 and acquired brains on PND 8. During this process, BrdU-labeled stem cells would continue to decline in proliferation as SW accumulated, therefore, eventually leading to a significant decrease in the number of $BrdU^+$ cells in GCL. This was a reasonable cause. Firstly, it may be because SW induced the apoptosis of neurons, just like the previous report (Lu et al., 2015). Secondly, we found that the level of NeuN, a neuron-specific nuclear protein, significantly reduced with SW treatment in hippocampus. Reelin, an extracellular matrix glycoprotein, regulates correct migration and positioning of postmitotic GCs from SGZ to GCL (Gong et al., 2007). We found that SW treatment increased the number of $NeuN^+$ and $Reelin^+$ cells in the hilus, indicating that newborn GCs did not migrate to their final destinations, GCL, according to previous studies (Ogawa et al., 2012; Tanaka et al., 2016). In addition, with SW exposure, the number of $GAD67^+$ cells in the hilus was not changed, but the number of $Reelin^+$ cells was increased. This is because GAD67 can mark almost all interneurons; while Reelin is the mark of only one type of interneuron, and the proportion is small (Houser, 2007).

Because about 90% of dentate GCs are generated after birth (Bayer, 1980), we labeled the newly generated GCs with GFP using postnatal *in vivo* electroporation to further investigate dendritic and axonal development of GCs in newborn pups with SW exposure to dams from GD 10 to PND 21. As described in the previous study (Ito et al., 2014), GFP-labeled cells could be shown to develop highly branched dendrites to the ML and thin and long axons in the hilus of DG. These morphological distinguishing features resembled normally developed GCs in DG. During the development of GFP-labeled GCs, they sprout highly branched dendrites that extended to the ML at PND 14–21 (Ito et al., 2014).

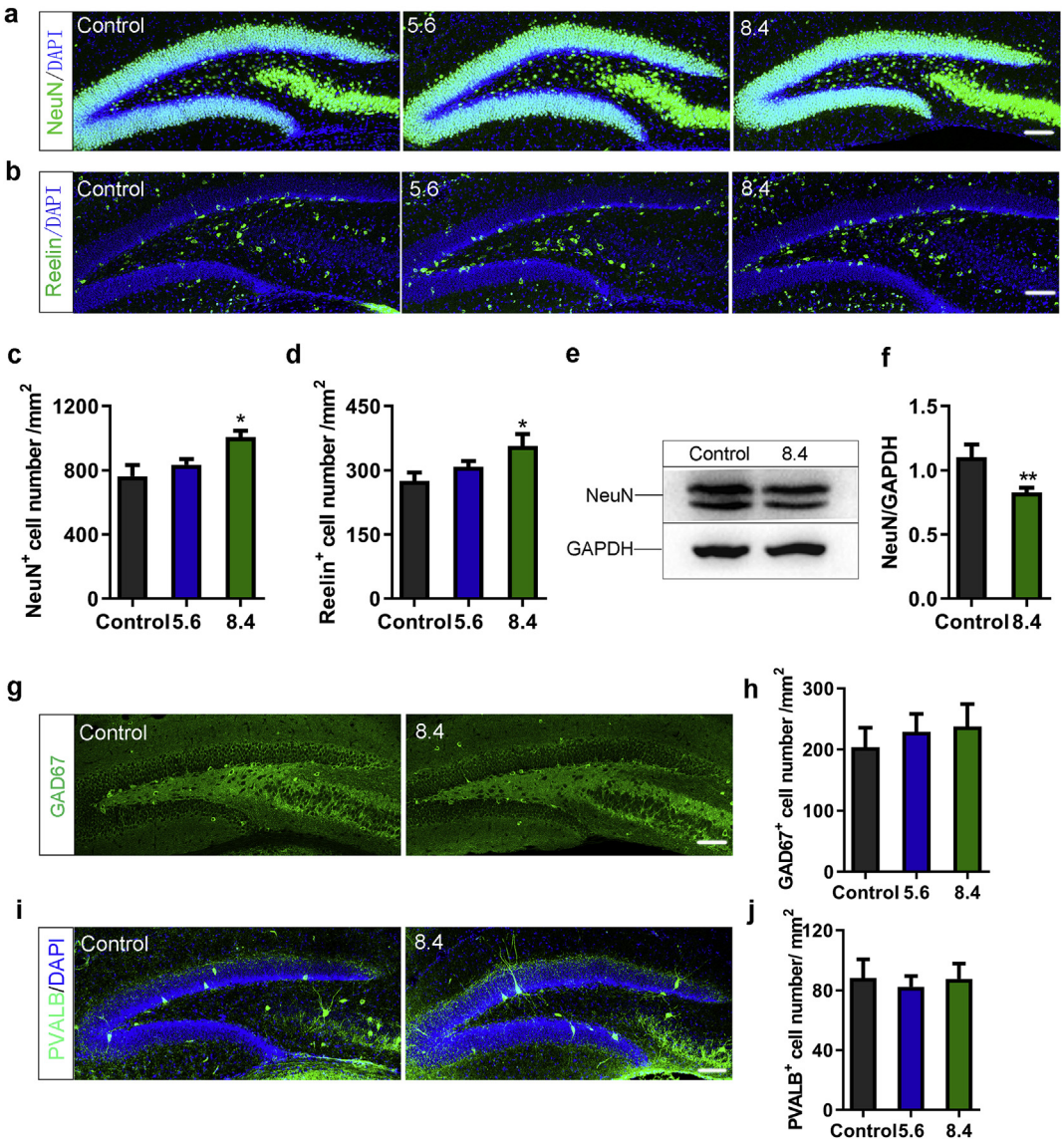

Fig. 5. The number of NeuN$^+$ cells and interneurons in the hippocampus at PND 21 after SW exposure during early postnatal development. **a-b** Immunostaining for hilar cells with NeuN or Reelin (green) and DAPI (blue) in the control and SW-treated groups. **c-d** Quantification of the number of NeuN$^+$ (**c**) and Reelin$^+$ (**d**) cells in the hilus. **e** Immunoblot analysis for NeuN expression levels after 8.4 mg/kg SW-treated hippocampus compared with control one. The GAPDH was used to control loading. **f** Quantification showing NeuN/GAPDH intensity ratios. **g, i** Images showed interneurons labeled by GAD67 or PVALB (green), respectively. Cell nuclei were counterstained with DAPI (blue). **h, j** Quantification of the number of GAD67$^+$ (**h**) and PVALB$^+$ (**j**) cells. Data were presented as mean ± SEM. $^*p < 0.05$ and $^{**}p < 0.01$ ($n = 9$ for each group). *Scale Bars* 100 μm in **a**, **b**, **g** and **h**.

We found that SW exposure significantly reduced the total length of dendrites and the number of terminal branch tips and influenced dendritic complex of GCs. These results indicate that during the postnatal development of GCs, SW impaired the dendritic development of GCs. And based on our previous study (Wang et al., 2015), we speculated that SW might affect the synaptic formation by GCs.

From birth until approximately 20 days of age, GCs elaborate their dendrites and come to receive afferent innervation (Fricke and Cowan, 1977; Loy et al., 1977). Thus, about at PND 20, the dentate gyrus is a location for forming an enormous number of synaptic connections. Studies have shown that the morphological classification of dendritic spines of GFP-labeled GCs can be obviously shown and the density of spines is similar to that by virus-mediated GFP-expressing (Ito et al., 2014; Zhao et al., 2006). In this study, we just analyzed the density of dendritic spines in the terminal branch of dendrites at ML at PND 21 and found no difference between the control group and SW-treated groups. However, the level of spinophilin, a marker for dendritic spine and one of post-synaptic components, declined with the exposure to SW. These results might be reasonable. The dendritic spine is not static but subject to change (Matsuzaki et al., 2004) and regulated by cytoskeleton, especially the balance between F-actin and G-actin (Okamoto et al., 2004). Thus spines change so quickly that they cannot be fully captured by images.

GCs of DG have thin and unmyelinated axons, the mossy fiber, and they form giant pre-synaptic boutons (MFB) impinging on large complex spines of the proximal dendrites of hilar mossy cells and CA3 pyramidal cells (Blackstad and Kjaerheim, 1961). Via mossy fiber synapses, GCs transmit afferent input from the entorhinal fibers to the hippocampus proper (Lisman, 1999). The enormous boutons (MFB, 2–5 μm in diameter) with the abundance of vesicles and the large number of release sites (Chicurel and Harris, 1992; Rollenhagen et al., 2007), strongly indicates that this synapse plays a vital role in the information flow within hippocampal tri-synaptic pathways (Sloviter and Lomo, 2012). This study showed that statistically, the density of MFB

was not affected by SW. And the expression level of synaptophysin, representing the number of synaptic vesicles at the end of the axon and one of presynaptic components, was not affected by SW. However, previous study has shown that SW can indeed affect the learning and memory of adult mice (Wang et al., 2015), which may be due to differences in age. It may also be that statistical methods need to be improved.

To summarize, SW inhibited the proliferation of RGCs and INPs and reduced the number of newborn dentate neurons, and decreased the developmental complexity of dendrites of GCs, resulting in the disorder of DG during the early postnatal development. And SW could affect neuronal migration and lead to hinder of the development of hippocampus. The toxicity of SW is attributed to its inhibition of acid or lysosomal α-mannosidase and Golgi α-mannosidase II (Cholich et al., 2009; Hueza and Gorniak, 2011; Kuntz et al., 2010). SW-mediated inhibition of Golgi α-mannosidase II is able to finally lead to abnormal increase of the synthesis of N-glycosylation (Tulsiani et al., 1988). And N-linked glycoproteins are widely distributed and play an important role in signal transduction, cell growth and migration and have important physiological functions in the central nervous system (Hueza and Gorniak, 2011). Our previous study also found that Fyn could arrest SW-induced apoptosis via the activity of Akt and its effective phosphorylation *in vitro* (An et al., 2015). There are still many other SW-poisoning mechanisms to be discovered to better control the locoweed. After all, locoweeds could be resistant to drought, cold, pests, and barren soil, which are the most prevalent poisonous plant in the grasslands.

Conflicts of interest

The authors declare no conflict of interest.

Acknowledgments

The work was supported by National Natural Science Foundation of China (No. 31572477 to S.Z.), Resource-based Industry Key Technology Project of Shaanxi Province, China (No. 2016KTCL02-19 to S.Z.), the Natural Science Foundation of Shaanxi Province, China (No. 2018JM3041 to X.Z.) and the Shenzhen Basic Research (Layout of Disciplines) Project Fund, China (JCYJ20170413154810633 to Y.W.).

Appendix A. Supplementary data

Supplementary data to this article can be found online at https://doi.org/10.1016/j.neuint.2019.104511.

References

Altman, J., Bayer, S.A., 1990a. Migration and distribution of two populations of hippocampal granule cell precursors during the perinatal and postnatal periods. J. Comp. Neurol. 301, 365–381. https://doi.org/10.1002/cne.903010304.

Altman, J., Bayer, S.A., 1990b. Mosaic organization of the hippocampal neuroepithelium and the multiple germinal sources of dentate granule cells. J. Comp. Neurol. 301, 325–342. https://doi.org/10.1002/cne.903010302.

An, L., Li, W.W., Cheng, G.C., 2015. Fyn arrests swainsonine-induced apoptosis in 293T cells via Akt and its phosphorylation. Genet. Mol. Res. 14, 5304–5309. https://doi.org/10.4238/2015.May.18.23.

Armien, A.G., Tokarnia, C.H., Peixoto, P.V., Barbosa, J.D., Frese, K., 2011. Clinical and morphologic changes in ewes and fetuses poisoned by Ipomoea carnea subspecies fistulosa. J. Vet. Diagn. Investig. 23, 221–232. https://doi.org/10.1177/104063871102300205.

Armien, A.G., Tokarnia, C.H., Peixoto, P.V., Frese, K., 2007. Spontaneous and experimental glycoprotein storage disease of goats induced by Ipomoea carnea subsp fistulosa (Convolvulaceae). Veterinary Pathology 44, 170–184. https://doi.org/10.1354/vp.44-2-170.

Bayer, S.A., 1980. Development of the hippocampal region in the rat. I. Neurogenesis examined with 3H-thymidine autoradiography. J. Comp. Neurol. 190, 87–114. https://doi.org/10.1002/cne.901900107.

Blackstad, T.W., Kjaerheim, A., 1961. Special axo-dendritic synapses in the hippocampal cortex: electron and light microscopic studies on the layer of mossy fibers. J. Comp. Neurol. 117, 133–159. https://doi.org/10.1002/cne.901170202.

Brunne, B., Franco, S., Bouche, E., Herz, J., Howell, B.W., Pahle, J., Mueller, U., May, P., Frotscher, M., Bock, H.H., 2013. Role of the postnatal radial glial scaffold for the development of the dentate gyrus as revealed by reelin signaling mutant mice. Glia 61, 1347–1363. https://doi.org/10.1002/glia.22519.

Byrnes, M.L., Reynolds, J.N., Brien, J.F., 2001. Effect of prenatal ethanol exposure during the brain growth spurt of the Guinea pig. Neurotoxicol. Teratol. 23, 355–364. https://doi.org/10.1016/s0892-0362(01)00150-7.

Campbell, C.E., Piper, M., Plachez, C., Yeh, Y.T., Baizer, J.S., Osinski, J.M., Litwack, E.D., Richards, L.J., Gronostajski, R.M., 2008. The transcription factor Nfix is essential for normal brain development. BMC Dev. Biol. 8, 52. https://doi.org/10.1186/1471-213X-8-52.

Chicurel, M.E., Harris, K.M., 1992. 3-Dimensional analysis of the structure and composition of CA3 branched dendritic spines and their synaptic relationships with mossy fiber boutons in the rat hippocampus. J. Comp. Neurol. 325, 169–182. https://doi.org/10.1002/cne.903250204.

Cholich, L.A., Gimeno, E.J., Teibler, P.G., Jorge, N.L., Acosta de Perez, O.C., 2009. The Guinea pig as an animal model for Ipomoea carnea induced alpha-mannosidosis. Toxicon 54, 276–282. https://doi.org/10.1016/j.toxicon.2009.04.012.

Dantas, A.F.M., Riet-Correa, F., Gardner, D.R., Medeiros, R.M.T., Barros, S.S., Anjos, B.L., Lucena, R.B., 2007. Swainsonine-induced lysosomal storage disease in goats caused by the ingestion of Turbina cordata in Northeastern Brazil. Toxicon 49, 111–116. https://doi.org/10.1016/j.toxicon.2006.08.012.

Driemeier, D., Colodel, E.M., Gimeno, E.J., Barros, S.S., 2000. Lysosomal storage disease caused by Sida carpinifolia poisoning in goats. Veterinary Pathology 37, 153–159. https://doi.org/10.1354/vp.37-2-153.

Dupret, D., Fabre, A., Doebroessy, M.D., Panatier, A., Rodriguez, J.J., Lamarque, S., Lemaire, V., Oliet, S.H.R., Piazza, P.-V., Abrous, D.N., 2007. Spatial learning depends on both the addition and removal of new hippocampal neurons. PLoS Biol. 5, 1683–1694. https://doi.org/10.1371/journal.pbio.0050214.

Ferreira, T.A., Blackman, A.V., Oyrer, J., Jayabal, S., Chung, A.J., Watt, A.J., Sjoestroem, P.J., van Meyel, D.J., 2014. Neuronal morphometry directly from bitmap images. Nat. Methods 11, 982–984. https://doi.org/10.1038/nmeth.3125.

Fricke, R., Cowan, W.M., 1977. An autoradiographic study of the development of the entorhinal and commissural afferents to the dentate gyrus of the rat. J. Comp. Neurol. 173, 231–250. https://doi.org/10.1002/cne.901730203.

Gong, C., Wang, T.-W., Huang, H.S., Parent, J.M., 2007. Reelin regulates neuronal progenitor migration in intact and epileptic hippocampus. J. Neurosci. 27, 1803–1811. https://doi.org/10.1523/jneurosci.3111-06.2007.

Hattiangady, B., Shetty, A.K., 2010. Decreased neuronal differentiation of newly generated cells underlies reduced hippocampal neurogenesis in chronic temporal lobe epilepsy. Hippocampus 20, 97–112. https://doi.org/10.1002/hipo.20594.

Hodge, R.D., Kowalczyk, T.D., Wolf, S.A., Encinas, J.M., Rippey, C., Enikolopov, G., Kempermann, G., Hevner, R.F., 2008. Intermediate progenitors in adult hippocampal neurogenesis: Tbr2 expression and coordinate regulation of neuronal output. J. Neurosci. 28, 3707–3717. https://doi.org/10.1523/jneurosci.4280-07.2008.

Houser, C.R., 2007. Interneurons of the dentate gyrus: an overview of cell types, terminal fields and neurochemical identity. Dentate Gyrus: a Comphrehensive Guide to Structure, Function, and Clinical Implications 163, 217–232. https://doi.org/10.1016/s0079-6123(07)63013-1.

Hueza, I.M., Gorniak, S.L., 2011. The immunomodulatory effects of Ipomoea cornea in rats vary depending on life stage. Hum. Exp. Toxicol. 30, 1690–1700. https://doi.org/10.1177/0960327110399477.

Ito, H., Morishita, R., Iwamoto, I., Nagata, K.-i., 2014. Establishment of an *in vivo* electroporation method into postnatal newborn neurons in the dentate gyrus. Hippocampus 24, 1449–1457. https://doi.org/10.1002/hipo.22325.

Jessberger, S., Zhao, C., Toni, N., Clemenson Jr., G.D., Li, Y., Gage, F.H., 2007. Seizure-associated, aberrant neurogenesis in adult rats characterized with retrovirus-mediated cell labeling. J. Neurosci. 27, 9400–9407. https://doi.org/10.1523/jneurosci.2002-07.2007.

Kadam, S.D., French, B.M., Kim, S.T., Morris-Berry, C.M., Zimmerman, A.W., Blue, M.E., Singer, H.S., 2013. Altered postnatal cell proliferation in brains of mouse pups prenatally exposed to IgG from mothers of children with autistic disorder[J]. J. Exp. Neurosci. 7, 93–99. https://doi.org/10.4137/JEN.S12979.

Kee, N., Teixeira, C.M., Wang, A.H., Frankland, P.W., 2007. Preferential incorporation of adult-generated granule cells into spatial memory networks in the dentate gyrus. Nat. Neurosci. 10, 355–362. https://doi.org/10.1038/nn1847.

Kempermann, G., Gage, F.H., 2002. Genetic influence on phenotypic differentiation in adult hippocampal neurogenesis. Dev. Brain Res. 134, 1–12. https://doi.org/10.1016/s0165-3806(01)00224-3.

Kempermann, G., Kuhn, H.G., Gage, F.H., 1997. More hippocampal neurons in adult mice living in an enriched environment. Nature 386, 493–495. https://doi.org/10.1038/386493a0.

Kuntz, D.A., Nakayama, S., Shea, K., Hori, H., Uto, Y., Nagasawa, H., Rose, D.R., 2010. Structural investigation of the binding of 5-substituted swainsonine analogues to golgi alpha-mannosidase II. Chembiochem 11, 673–680. https://doi.org/10.1002/cbic.200900750.

Li, G., Kataoka, H., Coughlin, S.R., Pleasure, S.J., 2009. Identification of a transient subpial neurogenic zone in the developing dentate gyrus and its regulation by Cxcl12 and reelin signaling. Development 136, 327–335. https://doi.org/10.1242/dev.025742.

Li, G.N., Pleasure, S.J., 2005. Morphogenesis of the dentate gyrus: what we are learning from mouse mutants. Dev. Neurosci. 27, 93–99. https://doi.org/10.1159/000085980.

Li, K., Cheng, X., Jiang, J., Wang, J., Xie, J., Hu, X., Huang, Y., Song, L., Liu, M., Cai, L., et al., 2017. The toxic influence of paraquat on hippocampal neurogenesis in adult mice. Food Chem. Toxicol. 106, 356–366. https://doi.org/10.1016/j.fct.2017.05.

067.
Li, Q., Wang, Y., Moldzio, R., Lin, W., Rausch, W.-D., 2012. Swainsonine as a lysosomal toxin affects dopaminergic neurons. J. Neural Transm. 119, 1483–1490. https://doi.org/10.1007/s00702-012-0827-6.
Lisman, J.E., 1999. Relating hippocampal circuitry to function: recall of memory sequences by reciprocal dentate-CA3 interactions. Neuron 22, 233–242. https://doi.org/10.1016/s0896-6273(00)81085-5.
Loy, R., Lynch, G., Cotman, C.W., 1977. Development of afferent lamination in the fascia dentata of the rat. Brain Res. 121, 229–243. https://doi.org/10.1016/0006-8993(77)90149-4.
Lu, H., Cao, D.D., Ma, F., Wang, S.S., Yang, X.W., Wang, W.L., Zhou, Q.W., Zhao, B.Y., 2014a. Characterisation of locoweeds and their effect on livestock production in the western rangelands of China: a review. Rangel. J. 36, 121–131. https://doi.org/10.1071/rj13105.
Lu, H., Ma, F., Zhang, L., Wang, J., Wu, C., Zhao, B., 2015. Swainsonine-induced apoptosis pathway in cerebral cortical neurons. Res. Vet. Sci. 102, 34–37. https://doi.org/10.1016/j.rvsc.2015.07.005.
Lu, H., Wang, S.-s., Wang, W.-l., Zhang, L., Zhao, B.-y., 2014b. Effect of swainsonine in Oxytropis kansuensis on golgi alpha-mannosidase II expression in the brain tissues of sprague-dawley rats. J. Agric. Food Chem. 62, 7407–7412. https://doi.org/10.1021/jf501299d.
Lu, H., Zhang, L., Wang, S.-s., Wang, W.-l., Zhao, B.-y., 2013. The study of the Oxytropis kansuensis-induced apoptotic pathway in the cerebrum of SD rats. BMC Vet. Res. 9. https://doi.org/10.1186/1746-6148-9-217.
Mathews, E.A., Morgenstern, N.A., Piatti, V.C., Zhao, C., Jessberger, S., Schinder, A.F., Gage, F.H., 2010. A distinctive layering pattern of mouse dentate granule cells is generated by developmental and adult neurogenesis. J. Comp. Neurol. 518, 4479–4490. https://doi.org/10.1002/cne.22489.
Mateus-Pinheiro, A., Alves, N.D., Sousa, N., Pinto, L., 2018. AP2γ: a new player on adult hippocampal neurogenesis regulation. J. Exp. Neurosci. 12, 1–4. https://doi.org/10.1177/1179069518766897.
Matsuzaki, M., Honkura, N., Ellis-Davies, G.C.R., Kasai, H., 2004. Structural basis of long-term potentiation in single dendritic spines. Nature 429, 761–766. https://doi.org/10.1038/nature02617.
Meijering, E., 2010. Neuron tracing in perspective. Cytometry 77A, 693–704. https://doi.org/10.1002/cyto.a.20895.
Ming, G.L., Song, H., 2011. Adult neurogenesis in the mammalian brain: significant answers and significant questions. Neuron 70, 687–702. https://doi.org/10.1016/j.neuron.2011.05.001.
Obeidat, B.S., Strickland, J.R., Vogt, M.L., Taylor, J.B., Krehbiel, C.R., Remmenga, M.D., Clayshulte-Ashley, A.K., Whittet, K.M., Hallford, D.M., Hernandez, J.A., 2005. Effects of locoweed on serum swainsonine and selected serum constituents in sheep during acute and subacute oral/intraruminal exposure. J. Anim. Sci. 83, 466–477.
Ogawa, B., Wang, L., Ohishi, T., Taniai, E., Akane, H., Suzuki, K., Mitsumori, K., Shibutani, M., 2012. Reversible aberration of neurogenesis targeting late-stage progenitor cells in the hippocampal dentate gyrus of rat offspring after maternal exposure to acrylamide. Arch. Toxicol. 86, 779–790. https://doi.org/10.1007/s00204-012-0801-y.
Okamoto, K.I., Nagai, T., Miyawaki, A., Hayashi, Y., 2004. Rapid and persistent modulation of actin dynamics regulates postsynaptic reorganization underlying bidirectional plasticity. Nat. Neurosci. 7, 1104–1112. https://doi.org/10.1038/nn1311.
Paxinos, G., Franklin, K.B.J., 2001. The Mouse Brain in Stereotaxic Coordinates, second ed. Academic Press, New York Deluxe.
Rollenhagen, A., Saetzler, K., Rodriguez, E.P., Jonas, P., Frotscher, M., Luebke, J.H.R., 2007. Structural determinants of transmission at large hippocampal mossy fiber Synapses. J. Neurosci. 27, 10434–10444. https://doi.org/10.1523/jneurosci.1946-07.2007.
Sloviter, R.S., Lomo, T., 2012. Updating the lamellar hypothesis of hippocampal organization. Front. Neural Circuits 6. https://doi.org/10.3389/fncir.2012.00102.
Squire, L.R., Zola-Morgan, S., 1991. The medial temporal lobe memory system. Science 253, 1380–1386. https://doi.org/10.1126/science.1896849.
Stegelmeier, B.L., James, L.F., Panter, K.E., Gardner, D.R., Pfister, J.A., Ralphs, M.H., Molyneux, R.J., 1999. Dose response of sheep poisoned with locoweed (Oxytropis sericea). J. Vet. Diagn. Investig. 11, 448–456. https://doi.org/10.1177/104063879901100510.
Stegelmeier, B.L., Molyneux, R.J., Elbein, A.D., James, L.F., 1995. The lesions of locoweed (astragalus-mollissimus), swainsonine, and castanospermine in rats. Veterinary Pathology 32, 289–298. https://doi.org/10.1177/030098589503200311.
Steiner, B., Klempin, F., Wang, L., Kott, M., Kettenmann, H., Kempermann, G., 2006. Type-2 cells as link between glial and neuronal lineage in adult hippocampal neurogenesis. Glia 54, 805–814. https://doi.org/10.1002/glia.20407.
Tanaka, T., Abe, H., Kimura, M., Onda, N., Mizukami, S., Yoshida, T., Shibutani, M., 2016. Developmental exposure to T-2 toxin reversibly affects postnatal hippocampal neurogenesis and reduces neural stem cells and progenitor cells in mice. Arch. Toxicol. 90, 2009–2024. https://doi.org/10.1007/s00204-015-1588-4.
Tulsiani, D.R., Broquist, H.P., James, L.F., Touster, O., 1988. Production of hybrid glycoproteins and accumulation of oligosaccharides in the brain of sheep and pigs administered swainsonine or locoweed. Arch. Biochem. Biophys. 264, 607–617. https://doi.org/10.1016/0003-9861(88)90327-x.
van Praag, H., Christie, B.R., Sejnowski, T.J., Gage, F.H., 1999. Running enhances neurogenesis, learning, and long-term potentiation in mice. Proc. Natl. Acad. Sci. U. S. A 96, 13427–13431. https://doi.org/10.1073/pnas.96.23.13427.
Wang, J., Song, L., Zhang, Q., Zhang, W., An, L., Zhang, Y., Tong, D., Zhao, B., Chen, S., Zhao, S., 2015. Exposure to swainsonine impairs adult neurogenesis and spatial learning and memory. Toxicol. Lett. 232, 263–270. https://doi.org/10.1016/j.toxlet.2014.11.017.
Wang, Y., Li, Y., Hu, Y., Li, J., Yang, G., Kang, D., Li, H., Wang, J., 2013. Potential degradation of swainsonine by intracellular enzymes of arthrobacter sp HW08. Toxins 5, 2161–2171. https://doi.org/10.3390/toxins5112161.
Wu, C., Wang, W., Liu, X., Ma, F., Cao, D., Yang, X., Wang, S., Geng, P., Lu, H., Zhao, B., 2014. Pathogenesis and preventive treatment for animal disease due to locoweed poisoning. Environ. Toxicol. Pharmacol. 37, 336–347. https://doi.org/10.1016/j.etap.2013.11.013.
Xu, C.-J., Wang, J.-L., Jin, W.-L., 2015. The neural stem cell microenvironment: focusing on axon guidance molecules and myelin-associated factors. J. Mol. Neurosci. 56, 887–897. https://doi.org/10.1007/s12031-015-0538-1.
Xu, M., Huang, Y., Li, K., Cheng, X., Li, G., Liu, M., Nie, Y., Geng, S., Zhao, S., 2018. Developmental exposure of decabromodiphenyl ether impairs subventricular zone neurogenesis and morphology of granule cells in mouse olfactory bulb. Arch. Toxicol. 92, 529–539. https://doi.org/10.1007/s00204-017-2059-x.
Young, D., Lawlor, P.A., Leone, P., Dragunow, M., During, M.J., 1999. Environmental enrichment inhibits spontaneous apoptosis, prevents seizures and is neuroprotective. Nat. Med. 5, 448–453. https://doi.org/10.1038/7449.
Yu, Y., Zhao, Q., Wang, J., Wang, J., Wang, Y., Song, Y., Geng, G., Li, Q., 2010. Swainsonine-producing fungal endophytes from major locoweed species in China. Toxicon 56, 330–338. https://doi.org/10.1016/j.toxicon.2010.03.020.
Zhao, C.M., Teng, E.M., Summers, R.G., Ming, G.L., Gage, F.H., 2006. Distinct morphological stages of dentate granule neuron maturation in the adult mouse hippocampus. J. Neurosci. 26, 3–11. https://doi.org/10.1523/jneurosci.3648-05.2006.